

STATUS AND CHALLENGES IN BEAM CRYSTALLIZATION*

Jie Wei[†] and Peicheng Yu, Department of Engineering Physics, Tsinghua University, China
 Hiromi Okamoto, Graduate School of Advanced Sciences of Matter, Hiroshima University, Japan
 Yosuke Yuri, Takasaki Advanced Radiation Research Institute, JAEA, Gumma, Japan
 Xiao-Ping Li, Skyworks Inc., USA
 Andrew M. Sessler, Lawrence Berkeley National Laboratory, USA

Abstract

During the past several decades, beam crystallization has been studied both theoretically and experimentally. Theoretical investigations have been numerical, mainly using computer modeling based on the method of molecular dynamics (MD), and analytical, based on phonon theory. Experimental investigations involve both ion storage rings and ion traps using both electron and laser beam cooling. Topics of interests include crystal stability in various accelerator lattices and under different beam conditions, colliding crystalline beams, crystalline beam formation in shear-free ring lattices with both magnets and electrodes, experimental simulation of alternating-gradient conditions with an ion trap, tapered cooling and coupled cooling, and beam dynamics at different temperature regime as the beam is cooled from high to low temperature. In this paper, we first review theoretical approaches and major conclusions pertaining to beam crystallization. Then, we analyze conditions and methods of the various major experiments. Finally, we discuss, both theoretically and experimentally, some improvements, open questions, and challenges in beam crystallization.

INTRODUCTION

Beam crystallization has been a topic of interests since first evidence of experimental anomaly was observed on an electron-cooled proton beam at the storage ring NAP-M [1]. Since then, strong space-charge dominated phenomena and one-dimensional (1-D) ordering states were reported with both proton and heavier ions at storage rings ASTRID [2], TSR [3], CRYRING [4], ESR [5], and S-LSR [6]. Electron and laser beam cooling methods were used in attaining such states. On the other hand, attempts to achieve beam ordering beyond 1-D have not been successful, unlike the situation with ion traps where multi-dimensional crystalline structures were attained [7].

Theoretically, two main approaches were pursued: for the low-temperature regime, the molecular dynamics (MD) method was used to predict the ground-state structure [8–11] and the low-temperature dynamics [11–13]; for the intermediate temperature, high density regime the more conventional beam dynamics methods including

envelope-equation resonance analysis [14, 15], space-charge particle-in-cell simulations, and intra-beam scattering analysis.

To attain an ordered state, effective beam cooling is needed to overcome beam heating caused by coherent resonance crossing and intra-beam scattering. Furthermore, the cooling force must conform to the dispersive nature of a crystalline ground state in a storage ring for 3-D structures. Experimentally, electron cooling has been used at NAP-M [1], ESR [4], CRYRING [5], and S-LSR [6] to cool beams of protons and heavier ions in all three directions, successfully reaching 1-D ordered states. With laser cooling, which has been used at ASTRID [2] and TSR [3], the beam can be cooled to ultra-low temperature in the beam rest frame in the longitudinal direction along the beam motion. However, to effectively reduce the transverse beam temperature methods like resonance coupling needs to be adopted [16]. With either cooling approach, the ideal “tapered cooling” effect is yet to be realized to move beyond 1-D ordering towards forming high-density crystalline structures in an actual storage ring.

CRYSTALLIZATION CONDITIONS

There are several necessary conditions for the formation of high-density, 3-D crystalline beams in storage rings.

Ground State Existence Condition

The storage ring is alternating-gradient (AG) focusing operating below the transition energy, γ_T ,

$$\gamma < \gamma_T \quad (1)$$

where γ is the Lorentz factor of the beam. This condition is due to the criterion of stable kinematic motion under Coulomb interaction when particles are subject to bending in a storage ring [11].

Phonon Spectrum and Resonance Condition

The bare transverse phase advances per lattice period need to be less than 90° , i.e.,

$$\nu_{x,y} < \frac{N_{sp}}{4} \quad (2)$$

where ν_x and ν_y are the bare horizontal and vertical tunes, and N_{sp} is the lattice super-periodicity of the storage ring. Note that the lattice elements consists of every device that

*Work supported by the “985 Project” of the Ministry of Education of China and the National Natural Science Foundation (10628510) and by the U.S. Department of Energy, Office of Basic Energy Sciences, under Contract No. DE-AC02-05CH11231.

[†]weij@tsinghua.edu.cn

interacts with the beam including magnetic fields (magnets), electric fields (accelerating and deflecting cavities), and cooling forces (cooling devices). This condition arises from the criteria that there is no linear resonance between the phonon modes of the crystalline structure and the machine lattice periodicity (requesting the left-hand-side of Eq. 2 to be less than $\sqrt{2}/4$) [13], and that linear resonance stopbands are not crossed during the entire cooling process as the 3-D beam density is increased [14, 15].

Cooling Force Condition

The cooling force needs to be applied in all three directions with cooling rates higher than the maximum heating rate of various mechanisms including intra-beam scattering, resonance heating, and diffusive processes, and the cooling force needs to conform to the dispersive nature of a crystalline structures, i.e. generally the cooling force needs to be “tapered” along the horizontal direction so that upon cooling particles’ momenta p_z is linearly proportional to their horizontal displacements x [12],

$$\Delta p_z = -f_z(p_z - C_{xz}x) \quad (3)$$

where p_z is the longitudinal momentum component, f_z indicates the cooling strength, and C_{xz} is the tapering factor dependent on the lattice property.

Relaxed Conditions for a Low-density Beam

The above mentioned conditions may be relaxed if the beam density in the storage ring is adequately low so that the crystalline ground state is 1-D or 2-D: the maximum bare transverse phase advances per lattice period may be relaxed, and tapered cooling may not be necessary. At low beam density, cooling rate needed to overcome intra-beam scattering heating is also low. Naturally, with conditions on the machine lattice (Eq. 2) and cooling force (Eq. 3) relaxed, 1-D ordering is the first step towards full-density 3-D crystallization.

CRYSTALLINE PROPERTIES

It is convenient to use normalized units to describe the equations of motion [11] so that the ordering state of the system is mainly described by the dimensionless temperature T . The dynamic is determined by the essential quantities like the beam energy γ and the storage ring parameters (strengths of the magnetic field, electric field, and cooling force). Quantities like the charge state and mass of the particles are contained in the normalization; they do not change the dynamics of the crystalline state.

Characteristic Length, Normalized Temperature

For a system of particles with charge Ze and mass Am_0 , the characteristic length ξ is given by [11]

$$\xi = \left(\frac{Z^2 r_0 \rho^2}{A \beta^2 \gamma^2} \right)^{1/3} \quad (4)$$

where $r_0 = e^2/4\pi\epsilon_0 m_0 c^2$ is the proton classical radius, βc and $\gamma Am_0 c^2$ are the velocity and energy of the reference particle, and ρ is the radius of curvature of the main bending region of the storage ring.

The normalized beam-frame temperature of the crystalline beam system is defined to be proportional to the deviations of momentum from their ground-state values, then squared and averaged over the distance and over all the particles [12]. For systems of 1-D crystalline ground state, this normalized temperature T is related to the conventional temperature T_B by the relation

$$T = \frac{k_B \rho^2}{Am_0 c^2 \beta^2 \gamma^2 \xi^2} T_B \quad (5)$$

where k_B is the Boltzmann constant. Components of the temperature T_B is related to storage ring laboratory-frame parameters by

$$k_B T_{Bx,y} = Am_0 c^2 \beta^2 \gamma^2 \left(\frac{\nu_{x,y}}{R_0} \right) \epsilon_{x,y} \quad (6)$$

$$k_B T_{Bz} = Am_0 c^2 \beta^2 \left(\frac{\delta p}{p} \right)^2 \quad (7)$$

where $\epsilon_{x,y}$ are the un-normalized rms emittance, and $\delta p/p$ is the rms momentum spread.

Ground State Structure

When all three conditions (Eqs. 1 – 3) are satisfied, the crystalline ground states can be reached. At these states, motion of the circulating particles is periodic in time with the period of the machine lattice. As shown in Fig. 1, particle trajectory in the transverse direction conforms to AG focusing (breathing), and in the longitudinal direction conforms to the change in bending radius (shear). In the presence of a longitudinal electric field, momentum p_z also varies periodically conforming to the energy gain at the cavity.

The ground state structure is a 1-D chain when the beam line density is low. The structure becomes 2-D lying in the plane of weaker transverse focusing if the line density λ in the machine is

$$\lambda > 0.62 \gamma \xi^{-1} [\min(\nu_y^2, \nu_x^2 - \gamma^2)]^{1/3} \quad (8)$$

For even higher density, the particles arrange themselves into 3-D crystals, becoming helices and then helices within helices. Fig. 2 shows such a multi-shell structure at a de-focusing location of the lattice. The maximum spatial density in the laboratory frame is approximately $\gamma \nu_y \sqrt{\nu_x^2 - \gamma^2} / (2\xi^3)$. If a sinusoidal electric field is present, the crystalline structure can be bunched azimuthally.

Beam and Lattice Heating

The minimum cooling rate needed for beam crystallization corresponds to the intra-beam scattering heating in an

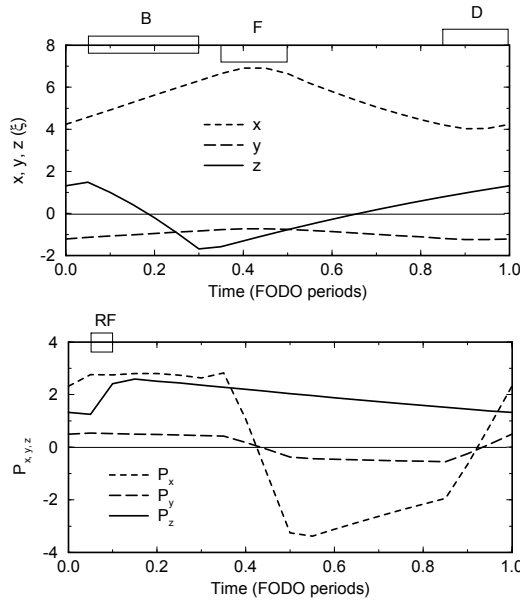


Figure 1: Particle trajectory of a bunched crystalline beam. The machine consists of 10 FODO cells with $\nu_x = 2.8$, $\nu_y = 2.1$, and $\gamma = 1.4$. Lattice components in each cell are displayed on the figure: B is a bending section, F and D are focusing and de-focusing quadrupoles, and RF is the bunching rf cavity.

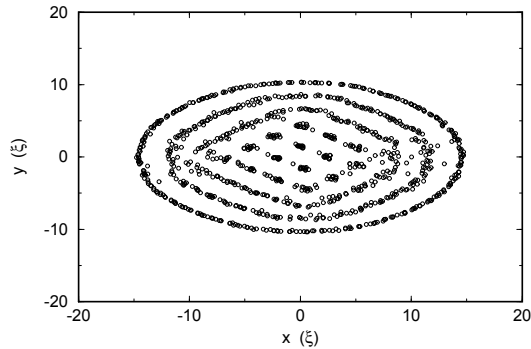


Figure 2: A multi-shell structure with particle positions projected into the $x - y$ plane ($\lambda = 25\gamma\xi^{-1}$).

AG-focusing lattice. At any non-zero temperature the beam absorbs energy and heats up under time-dependent external forces caused by variations in lattice focusing and bending. In the high temperature limit, this intra-beam scattering results in a growth rate proportional to $\lambda T^{-5/2}$. The peak heating rate occurs at the temperature of about $T \approx 1$ when the ordering starts to occur, as shown in Fig. 3. Typically, strong spatial correlation appears in all directions when the temperature is below $T \approx 0.05$. Lattice shear and AG focusing have similar effects on beam heating. Heating behavior is similar for both bunched and coasting beams. Effects of machine lattice imperfection, ion neutralization, and envelope instability have been studied.

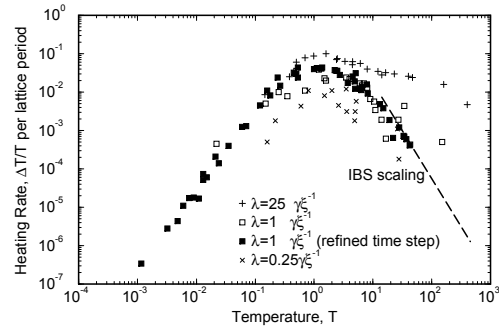


Figure 3: Typical heating rates as functions of temperature obtained by MD simulation at various line densities λ .

Cooling Methods

In order to attain a crystalline state, the beam must be effectively cooled in 3-D with a sufficient speed to overcome the heating. Both electron and laser cooling provide high cooling efficiency in the longitudinal direction but not in the transverse directions. ‘‘Sympathetic cooling’’ due to intra-beam scattering does produce transverse cooling. Coupling cavities operating on a synchro-betatron resonance or regular rf cavities in a dispersive region can provide effective 3-D cooling [16]. Realization of crystalline beams requires cooling that provides the ions with constant angular velocity, rather than constant linear velocity (tapered cooling) [12].

EXPERIMENTAL OBSERVATIONS

Experimental efforts on beam cooling and crystallization were made at several storage rings including NAP-M [1], TSR [3], ASTRID [2], ESR [4], CRYRING [5], and S-LSR [6]. In this section, we review the experimental results and provide theoretical estimates.

Table 1 lists experimental parameters and observations of these storage rings. All the experiments were performed at beam energies below transition (Eq. 1). On the other hand, every machine violates the crystallization condition Eq. 2. Furthermore, cooling forces were applied without a tapering factor (Eq. 3). Therefore, we do not expect the formation of 3-D crystalline states in these experiments.

With ASTRID and TSR, laser cooling was used to reduce the longitudinal temperature to a low level. Even though the longitudinal temperature could be extremely low, there was no clear indication of ordering aside from some anomaly in the longitudinal Schottky signal. With NAP-M, ESR, CRYRING, and S-LSR, electron cooling was used to cool the beam three dimensionally. A clear signature of these experiments was an abrupt drop of the momentum spread (and the longitudinal Schottky signal level) of the electron-cooled beam to very low values when the particle number decreased in the storage ring indicating possible ordering towards a 1-D chain in the longitudinal direction even though the transverse temperature may still be high. Not surprisingly, proton and heavier ion beams

Table 1: A compilation of experimental parameters and observations at existing storage rings.

	NAP-M	TSR	ASTRID	ESR	CRYRING	S-LSR
E_u [MeV/u]	65.7	2.43	0.00417	400	7.4	7
Circumference	47.25	55.4	40	108.36	51.63	22.557
γ	1.07	1.003	1.00000444	1.43	1.00789	1.00746
γ_T	1.18	2.96	4.34	2.6	2.33	1.41
N_{sp}	4	2	4	6	6	6
$\frac{\nu_x}{N_{sp}} / \frac{\nu_y}{N_{sp}}$	0.34 / 0.32	1.29 / 1.11	0.66 / 0.28	0.38 / 0.38	0.38 / 0.38	0.27 / 0.2 §
Species	Proton	$^3\text{Be}^+$	$^{24}\text{Mg}^+$	$^{238}\text{U}^{92+}$	$^{129}\text{Xe}^{36+}$	Proton
Cooling Method	EC	LC	LC	EC	EC	EC
ξ [μm]	4.61	5.1	21.8	12.7	11.2	4.83
$T_{Bx,y} / T_{Bz}$ [K] *	50 / 1	-- / 6	1000 / 0.001	10.8 / 57.9	11.6–34.8 / 0.58–1.74	5.7 / 0.31
$T_{x,y} / T_z$	13.9 / 0.28	-- / 1.84	1300 / 0.0013	0.001 / 0.005	0.006–0.018 / 0.0003–0.0009	1.67 / 0.09
N_0 (anomaly) †	2×10^7	--	5.5×10^8	1000	1000–10000	2000
N_0 (1-D to 2-D) ‡	6.0×10^6	1.2×10^7	1.2×10^6	7.8×10^6	4.7×10^6	3.3×10^6
Observations	Schottky anomaly	Indirect transverse cooling	Schottky anomaly	1-D ordering	1-D ordering	1-D ordering

* $T_{Bx,y,z}$: the observed lower temperature limit of the corresponding ion species in the machine.

† N_0 (anomaly): the ion number when anomalies in the Schottky signal were observed.

‡ N_0 (1-D to 2-D): the theoretical estimate (Eq. 8) of the intensity threshold when the ground state structure changes from 1-D to 2-D.

§ ν_x/N_{sp} and ν_y/N_{sp} of the S-LSR can be made to be below 0.25 simultaneously.

exhibited similar behaviors.

NAP-M

When the proton beam was electron-cooled to reach a steady state, the momentum spread of the beam was measured from the Schottky bandwidth. As the number of protons N_0 in the machine varied from 10^8 to 2×10^6 [1], the momentum spread first decreased with the decreasing beam intensity. However, when N_0 was reduced to 2×10^7 , the equivalent momentum spread became independent of the beam intensity.

MD study [17] indicates that at the intensity of $N_0 = 2 \times 10^7$ the ground state is 3-D. The observed Schottky anomaly thus does not correspond to ordering. In fact, at intensities higher than the anomaly point the scaling between the momentum spread and intensity indicated the equilibrium between intra-beam scattering and electron cooling. At intensities below the anomaly point, the observed constant momentum spread (Schottky signal) could be due to machine hardware issues [18].

On the other hand, the NAP-M machine lattice is appropriate for the formation of 1-D ordered states, should N_0 be below about 6×10^6 .

TSR

TSR was the first storage ring where longitudinal laser cooling was applied on an ion beam. Transverse cooling was achieved indirectly through intra-beam scattering [3]. A drawback of the TSR machine lattice is its low lattice periodicity. Even though theoretically 1-D or 2-D ordering (a transversely rotating zig-zag structure with periodicity of the machine lattice) may be formed [17], in practice the

large phase advance per lattice period makes beam crystallization nearly impossible.

ASTRID

At ASTRID, extremely low ($T_{Bz} \sim 1$ mK) temperature was achieved longitudinally through laser cooling [2]. Anomalies in Schottky signal were observed. However, the transverse temperature was too high to allow the formation of ordered structures during the experiments. MD studies indicate that 1-D and 2-D crystals may be formed if transverse temperature is reduced [17].

ESR

Systematic electron cooling studies were performed at ESR with various types of ion species at different densities [4]. For highly charged ions (Ar^{18+} and above), the momentum spread of the cooled ions dropped abruptly to very low values when the particle number in the machine decreased to 10000 and less indicating 1-D ordering in the longitudinal direction [19].

CRYRING

Ordering phenomena similar to those at ESR were observed at CRYRING [5]. Even though the beam energy is quite different, both lattice properties and predicted crystalline properties are similar.

S-LSR

Among the machines listed in Table 1, lattice design of the newly constructed and commissioned S-LSR is best suited for beam crystallization [6]. With the proton beam,

similar 1-D ordering phenomena were observed: the momentum spread of the cooled protons dropped abruptly to very low values when the particle number in the machine decreased to 2000 and less [20].

The bare transverse phase advance per period of lattice main magnets can be made to be below 90° . However, condition of Eq. 2 is rigorously satisfied only if rf cavities, cooling stations, and deflecting cavities are all placed symmetrically.

DISCUSSIONS AND SUMMARY

During the past three decades, both experimental and theoretical efforts were made in attaining crystalline beams in storage rings. Experimentally, states of 1-D ordering were realized using electron cooling on both proton and heavier ion beams at low density. Higher density, 3-D crystalline structures were only realized in ion traps; efforts to form 3-D crystalline beams in storage rings have not been successful. Theoretical approaches based on the molecular dynamics method and phonon spectrum analysis at low temperature and beam envelope resonance analysis at higher temperature were adequate in understanding the basic experimental findings of most machines (except for NAP-M case). More comprehensive analysis is needed especially for the intermediate temperature regime, and on the modeling of various cooling processes.

Challenges in beam crystallization are to design and construct storage rings with high lattice periodicity and low transverse phase advance (Eq. 2) to avoid linear resonances, and to implement effective beam cooling that conforms to the dispersive nature of the beam (Eq. 3).

Difficulties in attaining crystalline beams are due to the stringent necessary conditions (Eqs. 1 – 3) originating from the beam dynamics in a circular accelerator. Attempts were made to effectively compromise these conditions. For example, machine lattices of high or imaginary transition energy γ_T were proposed so that high-energy or colliding crystals may be realized in storage rings of moderate circumference [21]. Shear-free ring lattices consisting of both magnets and electrodes were designed at S-LSR so that 3-D crystalline structures may be formed without using tapered cooling forces [22].

Ion traps have been used to experimentally simulate features of an AG-focusing storage ring [23]. Combination of a storage ring and an ion trap may simulate the environment of colliding crystals.

Some fundamental questions remain to be answered. Crystalline beam corresponds to a new state of matter of one-component plasma where particles are confined by a periodic, time-dependent external potential with finite transverse boundary. Basic condensed-matter physics of such a system including phase-transition properties remains to be studied.

We thank H. Danared, N. S. Dikanski, D. Habs, J. S. Hangst, A. Noda, V. V. Parkhomchuk, and M. Steck for discussions on experimental results at various storage rings.

REFERENCES

- [1] E.E. Dement'ev et al, Zh. Tekh. Fiz. 50 (1980) 1717; N.S. Dikanskii, D.V. Pestrikov, Proc. Workshop on Electron Cooling and Related Applications, KfK 3846 (1984); V.V. Parkhomchuk, A.H. Skrinsky, Reports on Progress in Physics, 54 (1991) 919
- [2] J.S. Hangst et al, PRL 67 (1991) 1238, Phys. Rev. Lett. 76, 1238 (1991); N. Madsen, et al, Phys. Rev. Lett. 83, 4301 (1999); J. S. Hangst, et al, Phys. Rev. Lett. 74, 86 (1995)
- [3] S. Schroder et al. Phys. Rev. Lett. 64, 2901 (1990); H.-J. Miesner et al, Phys. Rev. Lett. 77, 623 (1996)
- [4] M. Steck et al, Phys. Rev. Lett. 77, 3803 (1996); M. Steck et al., Nucl. Instrum. Meth. A 532, 357 (2004)
- [5] H. Danared et al, Phys. Rev. Lett. 88, 174801 (2002)
- [6] T. Shirai et al. Phys. Rev. Lett. 98, 204801 (2007); T. Shirai et al., Proc. Workshop on Beam Cooling and Related Topics, Bad Kreuznach (2007) 139
- [7] F. Diedrich et al., Phys. Rev. Lett. 59, 2931 (1987); D. J. Wineland et al., Phys. Rev. Lett. 59, 2935 (1987); M. Drewsen et al, Phys. Rev. Lett. 81, 2878 (1998); T. Schätz, et al, Nature (London) 412, 717 (2001); U. Schramm et al, Nucl. Instrum. Meth. A 532, 348 (2004)
- [8] J.P. Schiffer, P. Kienle, Z. Phys. A 321, 181 (1985); J.P. Schiffer, O. Poulsen, Europhys. Lett. 1, 55 (1986)
- [9] A. Rahman, J. P. Schiffer, Phys. Rev. Lett. 57, 1133 (1986)
- [10] R.W. Hasse, J.P. Schiffer, Ann. Phys. 203 (1990) 419
- [11] J. Wei, X.-P. Li, A. M. Sessler, Phys. Rev. Lett. 73, 3089 (1994)
- [12] J. Wei, H. Okamoto, A. M. Sessler, Phys. Rev. Lett. 80, 2606 (1998)
- [13] X.-P. Li et al, Phys. Rev. ST-AB, 9, 034201 (2006)
- [14] I. Hofmann, J. Struckmeier, Proc. Workshop on Crystalline Ion Beams (1988) 140; B. Yang et al, Phys. Plasmas, 3, 688 (1996)
- [15] K. Okabe, H. Okamoto, Jpn. J. Appl. Phys. 42, 4584 (2003)
- [16] H. Okamoto, A. M. Sessler, and D. Möhl, Phys. Rev. Lett. 72, 3977 (1994)
- [17] J. Wei et al, in "Crystalline Beams and Related Issues", ed. D.M. Maletic A.G. Ruggiero, World Scientific (1996) p. 229; J. Wei, X. P. Li, A. M. Sessler, Proc. 1995 Part. Accel. Conf., (1995) 2946
- [18] Similarly, a constant level of momentum spread (Schottky signal) was observed at ESR for low intensity beams. The phenomena were attributed to the stability issues of the magnet power supply [4].
- [19] R. W. Hasse, Phys. Rev. Lett. 83, 3430 (1999); H. Okamoto et al, Phys. Rev. E 69, 066504 (2004)
- [20] A. Noda et al, New J. Phys. 8, 288 (2006)
- [21] J. Wei et al, Proc. Workshop on Beam Cooling and Related Topics, Bad Kreuznach (2007) 91
- [22] M. Ikegami et al., Phys. Rev. ST-AB 7, 120101 (2004)
- [23] H. Okamoto, Y. Wada, R. Takai, Nucl. Instrum. Meth. A 485 (2002) 244